Generating Square Wave by use of the HLIGN Equations in Deep Water

Lin He[1], **Binbin Zhao**[1,*], **Masoud Hayatdavoodi**[2], **R. Cengiz Ertekin**[1,3]

1 College of Shipbuilding Engineering, Harbin Engineering University, 150001 Harbin, China
2 School of Science and Engineering, University of Dundee, Dundee DD1 4HN, UK
3 Department of Ocean & Resources Engineering, University of Hawai'i, Honolulu, HI 96822, USA
zhaobinbin@hrbeu.edu.cn

1 Introduction

A sea state with two wave systems traveling at oblique angles is called cross sea [1]. Hwung and Tsai [2] found through calculations that the maximum heights of common waves exceed those predicted by energy superposition. However, their research primarily focuses on intermediate water depth conditions, and studies on deep-water crossing waves remain relatively scarce.

A square wave formed by two single waves intersecting at a 90° angle are a type of cross sea. A square wave in deep water is shown in Fig. 1.

Figure 1: A square wave in deep water [3].

Currently, the maximum crest height of square wave formed by the superposition of two regular waves in deep water, with equal wavelengths and wave heights at a 90° angle, remains unknown.

The Irrotational Green-Naghdi (IGN) equations were derived by Kim et al. [4, 5] using Hamilton's principle, and were later enhanced by Duan et al. [6] to facilitate the simulation of highly nonlinear deep-water waves by use of the HLIGN equations that are well-suited for studying strongly nonlinear waves in deep water.

This study by use of the HLIGN equations in deep water investigates how the crest height of square wave depends on the wave steepness of their individual components.

2 HLIGN Deep-Water Equations

In this work, we assume an inviscid and incompressible fluid and irrotational flow and the water mass density ρ is constant. We use a right-handed coordinate system with Oz directed upward, Ox to the right and Oy into the paper. The undisturbed free surface lies in the (x, y)-plane. Assume that the stream function is denoted by $\mathbf{\Psi}$, and the velocity components of a particle in the directions Ox, Oy, Oz, respectively, are given by u, v, w. The three-dimensional stream function can be expressed as $\mathbf{\Psi}(x, y, z, t)$ [4, 5, 7, 8],

$$\mathbf{\Psi}(x, y, z, t) = \sum_{m=1}^{K} \mathbf{\Psi}_m(x, y, t) f_m(z), \tag{1}$$

where $m = 1, \ldots, K$ denotes the level of the HLIGN equations, $\mathbf{\Psi}_m$ represents the stream function accounting solely for the $x-$ and $y-$ directions, and $f_m(z)$ is the vertical velocity component of the stream function given as [8]

$$f_m(z) = z^{m-1} e^{k_a z}, \tag{2}$$

where k_a is the representative wave number.

In Eq. (1), the velocity components can be expressed by [5]

$$(u, v) = \sum_{m=1}^{K} f'_m(z)\boldsymbol{\Psi}_m(x, y, t), \tag{3a}$$

$$w = -\sum_{m=1}^{K} f_m(z)\nabla \cdot \boldsymbol{\Psi}_m(x, y, t), \tag{3b}$$

where $f'_m(z)$ is the derivative of the vertical velocity component of the stream function, and ∇ denotes the gradient operator.

For Eq. (3), the unit energy, and E_k can be expressed by use of the Hamiltonian principle as [5]

$$E_k = \frac{1}{2}\int_{-\infty}^{\eta} \left(u^2 + v^2 + w^2\right) dz. \tag{4}$$

Thus, the HLIGN free surface equilibrium equation is written as

$$\frac{\partial}{\partial t}\left[\frac{1}{f_m(0)}\left(-\nabla\frac{\partial E_k}{\partial(\nabla\cdot\boldsymbol{\Psi}_m)} + \frac{\partial E_k}{\partial \boldsymbol{\Psi}_m}\right)\right] - \nabla\left(-g\eta - \nabla\cdot\frac{\partial E_k}{\partial(\nabla\eta)} + \frac{\partial E_k}{\partial\eta}\right) = 0, \tag{5}$$

where g is the gravitational acceleration, and η is the free surface measured from the still-water level. In this study, level V HLIGN equations are utilized.

3 Three-Dimensional Square Wave Numerical Simulations

In this section, the parameters of the three-dimensional square wave tank are presented. Simulations and analyses are conducted for three cases of three-dimensional square wave, with nonlinearity increasing progressively from weak to strong.

3.1 Simulation Cases for Square Wave

A square wave consists of waves propagating in two different directions. The numerical representation of the wave field is shown in Fig. 2.

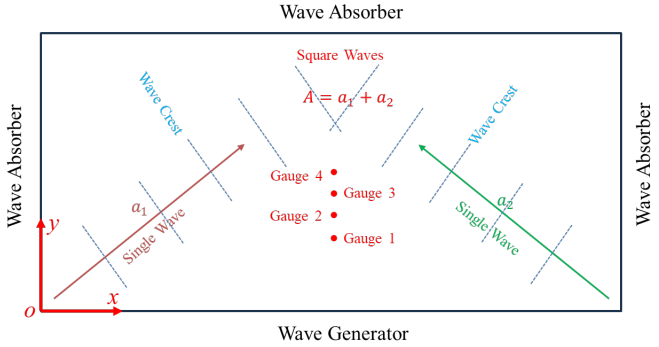

Figure 2: Configuration of the numerical wave field.

In the numerical calculations, to reduce the reflection of waves from the boundaries, wave absorption boundaries are applied on all sides except on the wave-generating side. Waves are generated at the wave generator boundary and propagate forward along the x-axis at angles θ_1, and θ_2, respectively, before being dissipated at the wave-absorbing boundary.

Consequently, the square wave is formulated as the sum of waves in these two directions:

$$\eta(x, y, t) = \sum_{i=1}^{2} a_i \cos\left[k_i(x\cos\theta_i + y\sin\theta_i) - \omega_i t\right], \tag{6}$$

where a_i is the wave amplitude, k_i and ω_i are the wave number and wave frequency, respectively, and θ_i denotes the wave propagation direction.

In the present study, the wave-maker is at $y = 0$. Four wave gauges are placed along the y-direction at $y = 1.5\lambda$, 2λ, 2.5λ, 3λ in the middle of tank to monitor the wave surface time history shown in Fig. 2. The wave surface time history at Gauge 3, is selected for nonlinear analysis.

Table 1: square wave conditions

Case	A (m)	H/λ	T (s)	k (1/m)	ω (rad/s)	θ (rad)
1	0.01	0.0032				
2	0.03	0.01	1.4185	2	4.42945	$\pi/2$
3	0.05	0.016				

In Table 1, the wave conditions considered in this study are presented, where H is the wave height of a single wave before the interaction, θ is the angle between the two waves at the point of intersection. Taking the cases in Table 1 as an example, two waves are generated, one with an angle of $\theta_1 = \pi/4$, another one with an angle of $\theta_2 = 3\pi/4$. Therefore, the angle θ is given by $\theta = \theta_2 - \theta_1 = \pi/2$. The linear solution can be obtained from Eq. (6).

3.2 Case 1

In Table 1, Case 1 exhibits weak nonlinearity, with the wave steepness of a single wave being approximately twice that of the simulated square wave. Therefore, the numerical results for this condition are expected to exhibit the smallest deviation from the linear solution. snapshot and time series of surface elevation are presented in Fig. 3.

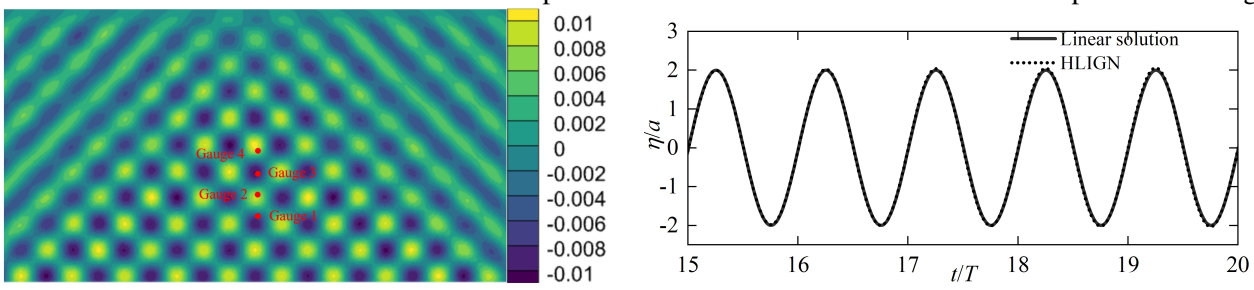

(a) snapshot in the three-dimensional wave field

(b) surface elevation recorded at Gauge 3

Figure 3: snapshot and time series of surface elevation for Case 1.

In Fig. 3a, the color bands represent the values of η, and also applied to Fig. 4a and Fig. 5a. As shown in Fig. 3b, due to the relatively weak wave nonlinearity, good agreement is observed between the HLIGN simulation results and the linear solution. Additionally, the crest height after the intersection of the two waves is found to be 2.01 times that of a single wave before the intersection.

3.3 Case 2

In this section, numerical simulations are performed for Case 2. As shown in Table 1, the wave steepness of a single wave in Case 2 is less than half that of the simulated square wave, indicating stronger nonlinearity compared to Case 1. snapshot and time series of surface elevation are presented in Fig. 4.

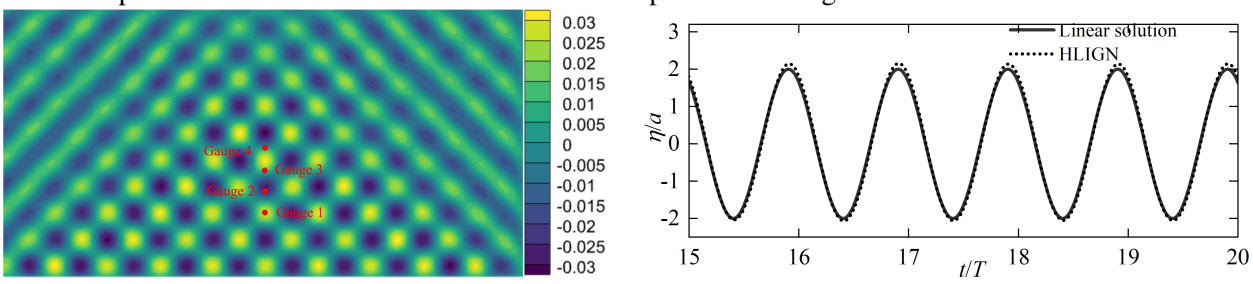

(a) snapshot in the three-dimensional wave field

(b) surface elevation recorded at Gauge 3

Figure 4: snapshot and time series of surface elevation for Case 2.

In Fig. 4a, waves propagating from two different directions form a regular, periodic square wave pattern near Wave Gauge 3. Due to the stronger nonlinearity in this case compared to Case 1, nonlinear effects causing deviations from the linear solution as observed in Fig. 4b. After the two waves intersect, the crest height reaches 2.09 times that of a single wave before the intersection.

3.4 Case 3

In this section, the square wave for Case 3 are simulated. As shown in Table 1, the wave steepness of the square wave in Case 3 is significantly greater than twice that of a single wave, indicating stronger nonlinearity compared to

the other two cases. snapshot and time series of surface elevation are presented in Fig. 5.

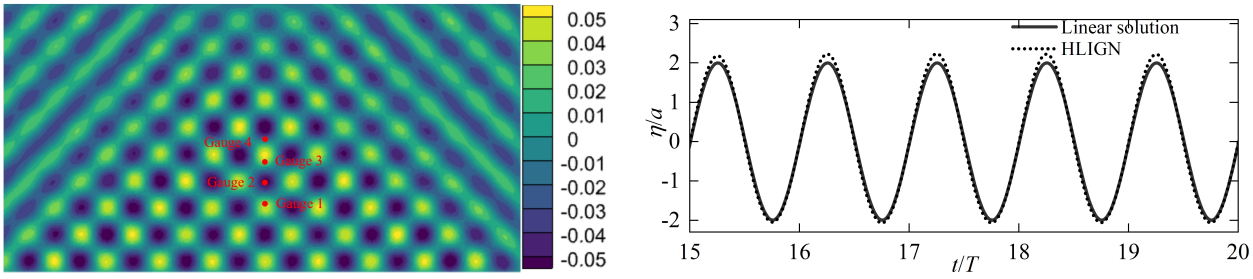

(a) snapshot in the three-dimensional wave field

(b) surface elevation recorded at Gauge 3

Figure 5: snapshot and time series of surface elevation for Case 3.

In Fig. 5a, the bidirectional crossing waves generated from the wave-generating boundary form a relatively regular square wave pattern near Gauge 3. At the intersection of two waves propagating from different directions, significantly stronger nonlinear effects are observed, with the crest height reaching 2.13 times that of a single wave, as shown in Fig. 5b.

4 Conclusions

This study conducted numerical simulations and analyses of square waves in a three-dimensional water tank by use of the HLIGN equations. The results show that when two waves intersect at a 90° angle to form a square wave, under weak nonlinearity, the HLIGN simulation results closely correspond to the linear solution. As nonlinearity increases, the HLIGN results exhibit increasingly pronounced nonlinear features compared to the linear solution.

In Case 1, the maximum crest height after the intersection of two waves is 2.01 times the crest height of a single wave before the intersection. With progressively stronger nonlinearity in Case 2 and Case 3, this quantity increases to 2.09 and 2.13, respectively. This study validated the ability of the HLIGN equations to simulate square waves under the deep-water conditions. Furthermore, the nonlinear analysis of square wave in deep water establishes a theoretical foundation for future, more comprehensive research on square wave by use of the HLIGN equations.

ACKNOWLEDGEMENT

This work is supported by the National Natural Science Foundation of China (No. 12172099) and the development and application project of ship CAE software.

REFERENCES

[1] Li, X. M., Susanne, L., Thomas, B., 2017. Is the Cross Sea Dangerous? European Space Agency, URL: `http://earth.esa.int/cgi-bin/confsea100415.html?abstract=349`.

[2] Hwung, H. H., Tsai, C. P., 1982. On the variation of characteristics of two wave trains crossing in intermediate depth. Coastal Engineering 1982, 862–886.

[3] Wendy, R., 2017. Rare Square-Shaped Waves In France Look Inviting, But They Can Be Dangerous. Elite Readers. URL: `https://www.elitereaders.com/rare-dangerous-square-shaped-waves/`.

[4] Kim, J. W., Ertekin, R. C., 2000. A numerical study of nonlinear wave interaction in regular and irregular seas: irrotational Green-Naghdi model. Marine Structures, 13, 331–347.

[5] Kim, J. W., Bai, K. J., Ertekin, R. C., Webster, W. C., 2001. A derivation of the Green-Naghdi equations for irrotational flows. Journal of Engineering Mathematics, 40, 17–42.

[6] Duan, W. Y., Zheng, K., Zhao, B. B., 2019. The Time Domain Simulations of the Improved HLIGN Model for Steep, Broadband Deep-water Ocean Waves. The Japan Society of Naval Architects and Ocean Engineers, 28, 171–175.

[7] Zhao, B. B., Zhang, T. Y., Duan, W. Y., Ertekin, R. C., Hayatdavoodi, M., 2019. Application of three-dimensional IGN-2 equations to wave diffraction problems. Journal of Ocean Engineering and Marine Energy, 5, 351–363.

[8] Webster, W. C., Zhao, B. B., 2018. The development of a high-accuracy, broadband, Green–Naghdi model for steep, deep-water ocean waves. Journal of Ocean Engineering and Marine Energy, 4, 273–291.